Atmospheric Research 232 (2020) 104677

Contents lists available at ScienceDirect

Atmospheric Research

journal homepage: www.elsevier.com/locate/atmosres

Consistent signal of aerosol indirect and semi-direct effect on water clouds in the oceanic regions adjacent to the Indian subcontinent

Sofiya Rao, Sagnik Dey*

Centre for Atmospheric Sciences, Indian Institute of Technology Delhi, New Delhi 110016, India

ABSTRACT

Quantifying aerosol-cloud interaction is one of the most challenging tasks in climate science. Previous studies in the oceanic regions adjacent to the Indian subcontinent providing evidence of aerosol impacts on cloud properties were mostly confined in the winter season. Here we analyze 15 years (March 2000–February 2015) of MODIS aerosol and cloud products and 10 years (October 2004–February 2015) of OMI absorbing aerosol index (AI) over the Arabian Sea (AS), Bay of Bengal (BoB) and South Indian Ocean (SIO) to examine the sensitivity of marine water cloud characteristics to changing aerosol loading. Amidst a monotonous increase in R_{eff} (cloud effective radius) with an increase in LWP (liquid water path) in clean and polluted conditions (an indicator of the meteorological influence), a smaller R_{eff} at higher AOD (aerosol optical depth) bins demonstrates that aerosol signal is detectable and consistent in LWP range of 150–350 g m^{-2}. Furthermore, a faster rate of R_{eff} growth with increasing LWP in clean condition and the pattern of change in cloud fraction (f_c) with an increase in AOD that cannot be explained by meteorology alone also provide evidence of the consistency of aerosol indirect effect. Evidence of aerosol semi-direct (decrease of LWP with an increase in AI) is also conspicuous in the AS and BoB. Our results suggest improved representations of aerosol and cloud processes in the models are required to reduce uncertainty in regional climate forcing.

1. Introduction

Poor understanding of the cloud feedback on climate is one of the major sources of uncertainty in climate forcing (Boucher et al., 2013). The problem remains unresolved due to the large discrepancy in representing cloud processes in the climate models (Lauer and Hamilton, 2013). Cloud microphysical and macrophysical properties evolve in response to changes in meteorology as well as aerosols (Wang, 2013; Rosenfeld et al., 2014; Altaratz et al., 2014). Aerosols serve as the cloud condensation nuclei (CCN) and therefore impact the cloud properties by enhancing the cloud albedo (R_c) and lifetime resulting in a negative forcing (Seinfeld et al., 2016). Absorbing aerosols on the other hand tend to decrease low cloud cover and liquid water path (LWP), resulting in a positive forcing (Johnson et al., 2004).

Impacts of aerosols on cloud characteristics via microphysical pathway are referred to as "indirect effects" (Altaratz et al., 2014). The aerosol indirect effect was first studied extensively during the Indian Ocean Experiment (INDOEX) (Ramanathan et al., 2001; Heymsfield and McFarquhar 2000). Subsequently, systematic studies were launched to examine the aerosol characteristics across the Indian subcontinent (a major regional aerosol hotspot) using ground-based measurements under various network programs such as AERONET (Eck et al., 2012) and ARFINET (Moorthy et al., 2013), and campaigns (e.g. Satheesh et al., 2009). In addition, specialized programs such as Continental Tropical Convergence Zone, CTCZ (Sengupta et al., 2013) and Cloud-Aerosol interaction and precipitation enhancement experiment, CAIPEEX (Kulkarni et al., 2012; Pandithurai, 2012) were launched to investigate aerosol-cloud interaction in the Indian region. These studies, no doubt, advanced our understanding about the role of aerosols on warm rain processes in the Indian region, but they are limited to a particular season.

To improve the representation of aerosol-cloud interaction in climate models, we need to ensure the consistency of aerosol signal (that is observed during the campaigns) over a longer period of time and larger region because such interaction is highly complex (Fan et al., 2016; Li et al., 2016). For long-term observations, we resort to satellite data. Previously, Chylek et al. (2006) analyzed Moderate Resolution Imaging Spectroradiometer (MODIS) data of five September (clean condition) and January (polluted condition) over the tropical Indian Ocean. They observed evidence of aerosol indirect effect for water clouds in the winter. Dey et al. (2011) have reported a transition from indirect to semi-direct effect in the Indian Ocean during the dry season of 2006–2007. These studies clearly showed evidence of aerosol-cloud interaction, but within the time of the year when aerosols are transported from the land to the ocean. Recently, Kant et al. (2019a) have investigated cloud radiative forcing modulation due to aerosol-induced changes in cloud characteristics over Indian region using satellite data. Precipitation mediated aerosol-cloud relationships are often called

* Corresponding author.
E-mail address: sagnik@cas.iitd.ac.in (S. Dey).

https://doi.org/10.1016/j.atmosres.2019.104677
Received 29 March 2019; Received in revised form 17 August 2019; Accepted 11 September 2019
Available online 12 September 2019

'lifetime effects', and stem from the hypothesis that changes in the concentration of aerosols present in clouds can alter precipitation efficiency of clouds, thereby changing the cloud fraction and, hence the radiative forcing of the climate system (Stevens and Feingold, 2009). Yet, it is not fully known under what conditions cloud characteristics are most sensitive to changes in aerosol properties. Stevens and Feingold (2009) suggested focusing on particular cloud types to obtain a robust signal of aerosol-cloud interaction.

Here we analyze 15 years (Mar 2000-Feb2015) of satellite-based aerosol and cloud products to understand the sensitivity of marine water cloud characteristics viz. cloud fraction (f_c), cloud optical depth (COD), effective radius of cloud droplets (R_{eff}) and liquid water path (LWP) to aerosol loading. Choice of the oceanic regions adjacent to the Indian subcontinent was driven by two factors – better accuracy of cloud and aerosol products of satellites over oceans than over land (Levy et al., 2013; Platnick et al., 2017) and larger seasonal variation in aerosol loading over the oceans than over the land (Dey and Di Girolamo, 2010). The potential importance of aerosol indirect and semi-direct effects in modulating cloud radiative forcing is also evident in shallow marine cloud systems (Liu et al., 2017). In this work, we provide evidence of aerosol indirect and semi-direct effects on marine water clouds consistently over a long period of time. The next section describes the satellite data and analysis, followed by interpretation and discussion of the results in the next section.

2. Approach

2.1. Study area

We focus our analysis over the Arabian Sea (AS) bounded within the Equator to 20° N latitude and 58–73° E longitude, the Bay of Bengal (BoB) bounded within the Equator to 20° N latitude and 86–94°E longitude, and the South Indian Ocean (SIO) bounded within 20°S latitude to the Equator and 58–94°E longitude (Fig. 1a) (Google maps, 2019). Aerosol characteristics in these three oceanic regions are quite different (Dey and Di Girolamo, 2010). While maritime aerosols are expected in any oceanic region, dust and anthropogenic aerosols are transported to the AS and BoB seasonally with a larger fraction of dust loading over the AS relative to the BoB due to its proximity to the source regions (Dey and Di Girolamo, 2010). This allows us to examine the sensitivity of marine cloud characteristics to changing aerosol loading in contrasting aerosol environments. Moreover, the accuracy of MODIS aerosol and cloud products is better over the ocean than over the land (Levy et al., 2013; Platnick et al., 2017. Therefore, detection of the aerosol signal is expected to be easier over the oceanic regions.

2.2. Satellite and meteorological data

MODIS (onboard NASA's TERRA satellite) collection 6 cloud and aerosol products (Levy et al., 2013) are analyzed in this work. MODIS products are archived at NASA DAAC website http://disc.sci.gsfc.nasa.gov/giovanni. MODIS measures the spectral radiance in 36 bands from visible to thermal infrared wavelengths (0.41 to 15 μm). MODIS cloud (Platnick et al., 2017) and aerosol products (Levy et al., 2013) are well-validated and used globally. For retrieving aerosol optical properties over the ocean the Dark target (DT) algorithm (Tanré et al., 1997). For this study, daily L3 aerosol optical depth (AOD) and cloud products for water clouds (i.e. f_c, CTP, R_{eff}, LWP and COD) at spatial resolution 1° × 1° are analyzed. We note that MODIS products have defined uncertainty range. For example, AOD has an uncertainty range of 0.03 ± 0.05AOD over the ocean (Remer et al., 2005). The uncertainty of R_{eff} is within the range of 1–3 μm for optically thick clouds (King et al., 1997; Kant et al., 2019b), while that of COD is in the range of 10–21% (Minnis et al., 2004; Sayer et al., 2016).

Absorbing Aerosol Index (AI) from Ozone Monitoring Instrument (OMI) for the period Oct 2004-Feb 2015 at similar spatial resolution 1° × 1° are analyzed to quantify absorbing aerosol loading (Torres et al., 2007). To ensure consideration of marine water clouds in the analysis, we restrict our analysis to clouds whose top pressure is below than 680 hPa.

We have used ERA-interim data for analysis of meteorological parameters such as SST (sea surface temperature) and RH (relative humidity) at 850 hPa (representative of the lower troposphere). ERA-Interim data (Noh et al., 2016) of resolution of 0.25° × 0.25° are regridded to 1° × 1° to match L3 MODIS products. We examine the behavior of f_c with an increase in SST and RH to understand the meteorological influence and to see if the observed f_c-AOD relation could be explained by meteorology alone (following similar approach of Dey et al., 2011).

2.3. Analysis to isolate aerosol signal

First, we examine the monthly climatology of aerosol and cloud properties in these regions by averaging daily data. Cloud albedo (R_c)

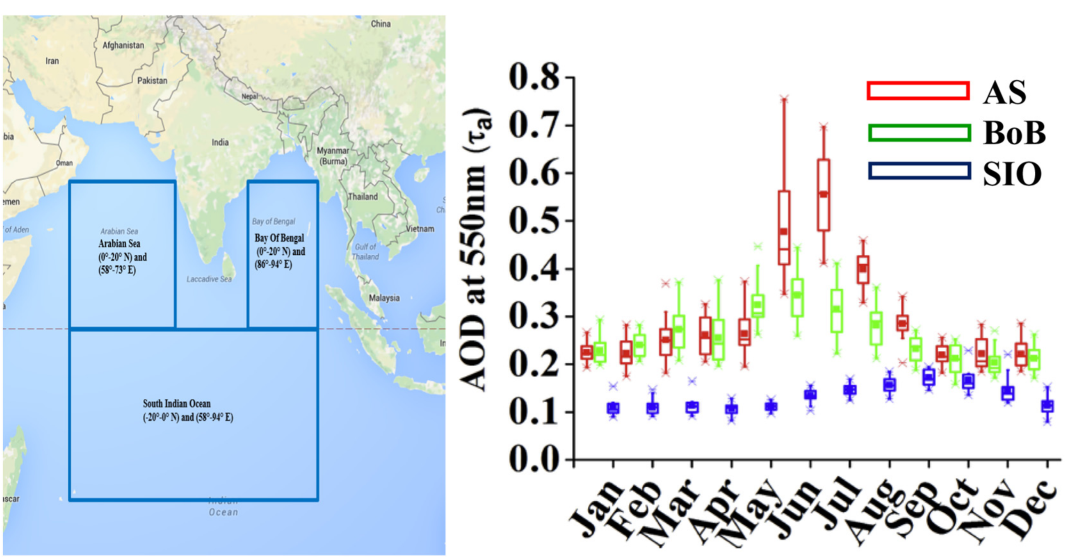

Fig. 1. (a) Study region (source: google maps) and (b) Monthly statistics of AOD at 550 nm for marine low clouds over the AS, BoB and SIO. Box plots show 5th and 95th percentile ranges.

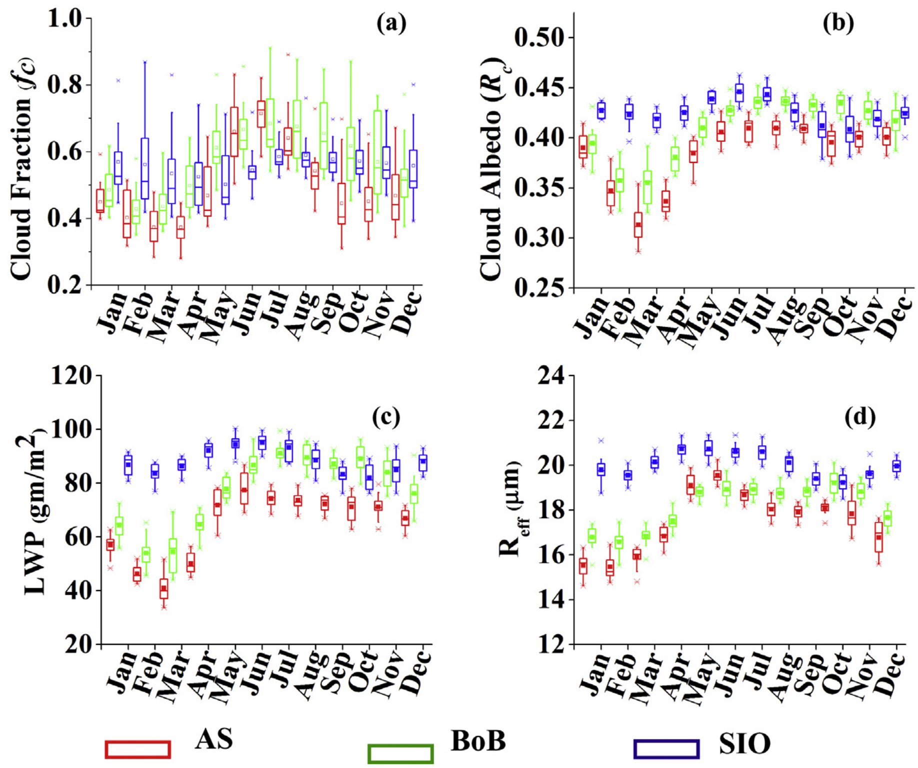

Fig. 2. Monthly statistics of (a) f_c, (b) R_c, (c) LWP and (d) R_{eff} for low clouds over the AS, BoB and SIO. Box plots show 5th to 95th percentile ranges.

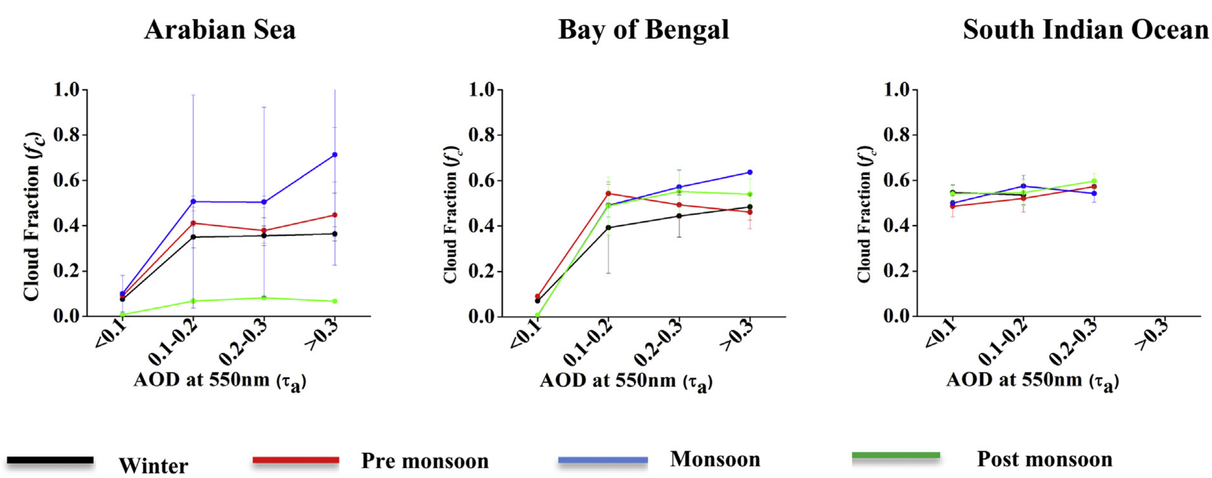

Fig. 3. Variation of f_c with an increase in AOD Error bars are ± 1σ.

has been calculated from COD following Seinfeld and Pandis (1998):

$$R_c = \frac{\text{COD}}{(\text{COD} + 7.7)}$$

For identifying the aerosol indirect effect, we take a two-fold analysis. First, we examine the changes in f_c in response to AOD and to meteorology. We adopt a binned approach where the cloud parameters for each individual grid are grouped in five AOD bins - AOD < 0.1 (very low pollution), 0.1 < AOD < 0.2 (low pollution), 0.2 < AOD < 0.3 (moderate pollution), 0.3 < AOD < 0.4 (moderately high pollution) and AOD > 0.4 (polluted condition). Though AOD values are observed as high as > 0.8 in the AS and BoB, we grouped them in AOD > 0.4 bin to ensure large enough sample size for each AOD bin; otherwise sample size would have been less at the higher (> 0.5) AOD bins compared to the lower (< 0.4) AOD bins biasing the results. Classical cloud physics (Seinfeld and Pandis, 1998) suggests that R_{eff} increases as a function of LWP because the availability of moisture would propel cloud droplet growth. We hypothesize that if the aerosol indirect effect exists, R_{eff} should be smaller at higher AOD bins at any given LWP because higher aerosol concentrations would lead to higher CCN inhibiting cloud droplet growth micro physically. Therefore, we analyze R_{eff} variation at every LWP bin of 50 g m^{-2} separately for each of the five AOD bins. Whether at a particular LWP bin R_{eff} at higher AOD is significantly lower than R_{eff} at lower AOD is examined with *t*-test.

The semi-direct effect explains that absorption of solar radiation by aerosols would increase the temperature of the surrounding air resulting in evaporation of cloud droplets (Hansen et al., 2007). Therefore, we hypothesize that if semi-direct effect prevails in our study region, LWP should reduce with an increase in absorbing aerosol loading provided that the aerosols and clouds are present around a similar altitude range. For quantifying absorbing aerosols, we consider three AI

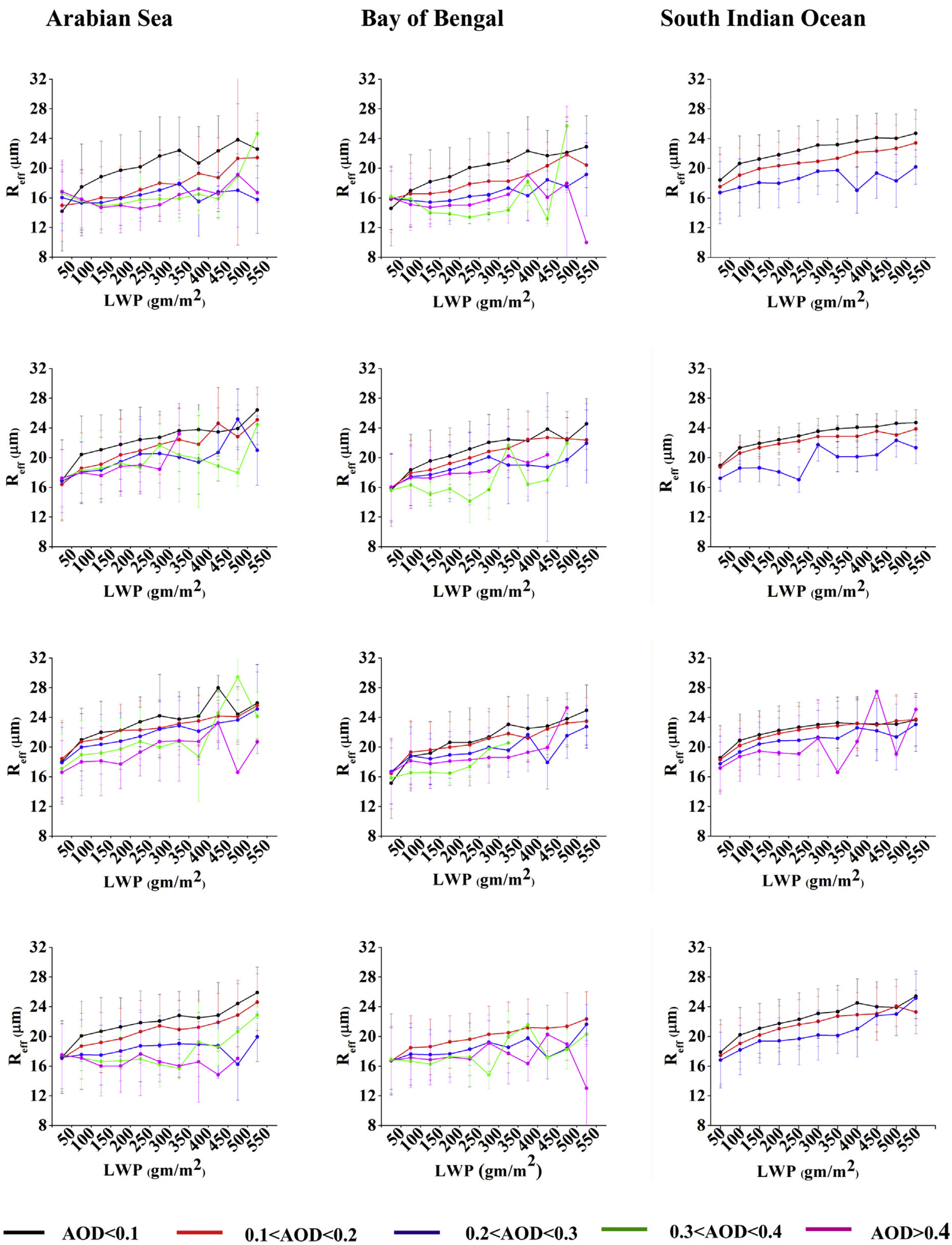

Fig. 4. Variation of R_{eff} (μm) with an increase in LWP (g m^{-2}) at five AOD bins, error bars are ± 1σ. The panels from the top represent winter, pre-monsoon, monsoon and post-monsoon seasons, respectively.

bins, AI < 1 (less absorbing), 1 < AI < 2 (moderately absorbing) and AI > 2 (highly absorbing).

Inter-relationships of various cloud parameters (described above) in view of the transition from low to high aerosol loading and from less absorbing to high absorbing aerosol loading are examined. We do not resort to "correlation approach" to establish causality, as it is difficult to disentangle the meteorological signal from the aerosol signal by looking at the correlation alone (Gryspeerdt et al., 2016; Christensen et al., 2017; Kant et al., 2019a). We only analyze low clouds to ensure co-existence of aerosols and clouds in the oceanic regions. The binned

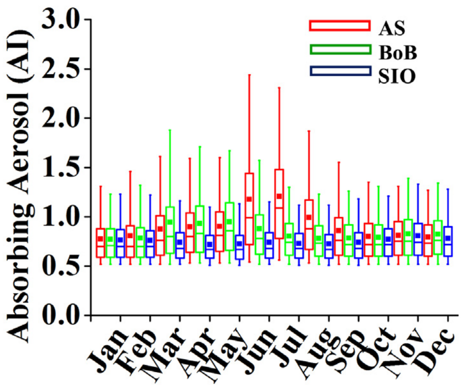

Fig. 5. Monthly statistics of AI over the AS, BoB and SIO. Box plots show 5th to 95th percentile ranges.

approach allows us examining the robustness of the aerosol signal if the relationships appear consistent over a range of AOD and AI bins simultaneously with meteorology signal. Though level 2 data would have provided better spatial resolution, we believe sample size (2,381,280, 1,948,320 and 5,195,520 samples over the AS, BoB and SIO, respectively) analyzed over 15 years period is large enough to detect the aerosol signal and its consistency.

3. Results

3.1. Climatology of aerosol and cloud characteristics in the oceanic regions adjacent to the Indian subcontinent

Fig. 1b illustrates 15-year AOD climatology over the study region. AOD shows strong seasonality over the AS and BoB and is also much higher than AOD in SIO. AOD over the AS and BoB is dominated by anthropogenic aerosols transported from the Indian landmass in the post-monsoon (October–November) and winter (December–February) seasons by northeasterly winds, while it is dominated by maritime aerosols and mineral dust transported from the central and west Asian arid regions in the pre-monsoon (March–May) and monsoon (June–-September) seasons with a larger dust load over the AS than the BoB due to its proximity to the source regions (Dey and Di Girolamo, 2010). During the monsoon, maritime aerosol production is enhanced due to stronger winds. On the contrary, the aerosol load is very low (AOD < 0.2) throughout the year over the SIO as it is far away from the anthropogenic source regions. AOD in the SIO is mostly dominated by maritime aerosols with the occasional contribution of biomass burning aerosols transported from the Indonesian archipelago (Duflot et al., 2011). Higher AAI is observed over the AS and BoB when anthropogenic aerosols are transported from the Indian landmass and dust aerosols are transported from the western arid regions. On the contrary, low AI is observed throughout the year in SIO as mentioned in Fig. 5.

Monthly climatology of the cloud characteristics (f_c, R_c, LWP and R_{eff}) is displayed in Fig. 2. f_c shows larger seasonality over the AS and BoB than over the SIO (Fig. 2a). During the post-monsoon to winter seasons, f_c over the SIO is higher than over the other two regions. As the summer monsoon approaches, the ITCZ migrates towards north and f_c starts increasing over the AS and BoB overtaking the SIO. Larger f_c over the BoB compared to the AS during the monsoon season may be attributed to warmer sea surface temperature (SST) in the BoB (Cherchi et al., 2007). Higher R_c is observed in the SIO during January–May relative to the other two regions (Fig. 1b). Monthly variation of R_c depends on COD, which in turn depends on LWP and R_{eff}. Clouds with larger LWP (having more cloud drops) and smaller R_{eff} reflect more solar radiation. However, the change in R_c with an increase in LWP and decrease in R_{eff} is nonlinear (Seinfeld and Pandis, 1998).

The pattern of monthly variation of LWP (Fig. 2c) and R_{eff} (Fig. 2d) follows the variation of R_c. LWP and R_{eff} in the SIO peak in May–June, but the seasonal amplitude is subdued. LWP remains in the range 80–100 g m^{-2} and R_{eff} in the range 18–21 μm in the SIO throughout the year. R_{eff} in the AS and BoB is in the range 14–19 μm and is smaller than R_{eff} in the SIO throughout the year, which hints at aerosol indirect effect as AOD is much lower in the SIO (Fig. 1b). This aspect is discussed in details in the next sub-section. While LWP is persistently high in the BoB than in the AS throughout the year, R_{eff} is slightly higher in the BoB than in the AS only during November–March and are comparable in the remaining months. Larger LWP is observed during southern hemispheric summer (northern hemispheric winter) in the SIO relative to the AS and BoB and larger LWP is observed in the BoB than in the AS during the summer monsoon season.

3.2. Consistency of aerosol indirect effect signal

First, we examine the variation of f_c with an increase in AOD over the three regions (top panel of Fig. 3). Here, f_c does not show any significant relation with AOD over the SIO. Over the other two oceanic regions, f_c usually increases with an increase in AOD in all the seasons. However, this increasing trend is not consistent. For example, f_c increase for AOD exceeding 0.2 is marginal over the AS (except in the monsoon season) and BoB. In fact, f_c either remains unchanged or decreases marginally at higher AOD bins. Previously, Dey et al. (2011) observed a transition from indirect to semi-direct effect for marine trade-wind cumulus clouds in the Indian Ocean during the winter season. If the semi-direct effect prevails, f_c should reduce with an increase in absorbing aerosol loading. In the winter season, higher AOD over the Indian Ocean usually implies an increase in absorbing aerosols (Dey et al., 2011). In our analysis here, we consider low clouds (i.e. stratocumulus and stratus along with cumulus). The semi-direct effect is most dominant for cumulus clouds. Hence, we do not observe a large decrease in f_c at higher AOD bins as observed by Dey et al. (2011), rather we observe f_c flattening out. We discuss the semi-direct effect separately in the next sub-section. We note that though cloud formation is favored in polluted regions, the observed-f_c relation is only indicative of aerosol indirect effect and not surety as AOD may be enhanced due to cloud contamination (Zhao et al., 2009; Christensen et al., 2017). Since we do not observe a monotonous increase in f_c with AOD, the major influence of cloud contamination is ruled out. However, high f_c influenced by meteorology may lead to high AOD (Gryspeerdt et al., 2016). f_c-SST and f_c-RH patterns (not shown here) do not show either monotonous increase or consistent pattern across the seasons, suggesting that meteorology alone cannot explain the observed f_c-AOD relation. Hence we also analyze R_{eff}-AOD-LWP relation in these regions so that both meteorological and aerosol signals can be detected simultaneously.

One of the key features of aerosol indirect effect is smaller R_{eff} in polluted condition (Albrecht, 1989), but this must satisfy the criteria that LWP remains more or less constant. Growth of cloud drops can be facilitated if moisture availability is abundant and this can partially (or completely) negate the impact of aerosols on cloud microphysics, where abundant aerosols present as CCN can reduce the size of cloud droplets, thereby suppressing the warm-rain process by inhibiting collision and coalescence process (Squires and Twomey, 1966; Warner and Twomey, 1967; Rosenfeld, 1999). We examine R_{eff}-LWP relation for five AOD bins (Fig. 4). Five key points emerge from this analysis. Firstly, R_{eff} increases with an increase in LWP for all AOD bins. Secondly, the rate of change of R_{eff} as a function of LWP is higher in clean condition (i.e. lower AOD) relative to the polluted condition. Availability of moisture at any given LWP bin to an individual cloud drop is larger in a clean condition relative to the polluted condition as fewer CCNs are expected in clean condition, thereby enhancing growth at a faster rate. Also, LWP would reduce if the clouds precipitate.

Polluted clouds with small R_{eff} precipitate less and this would maintain high LWP at lower R_{eff} thereby flattening the R_{eff}-LWP curve at higher AOD. Thirdly, R_{eff} is smaller in high AOD not throughout every

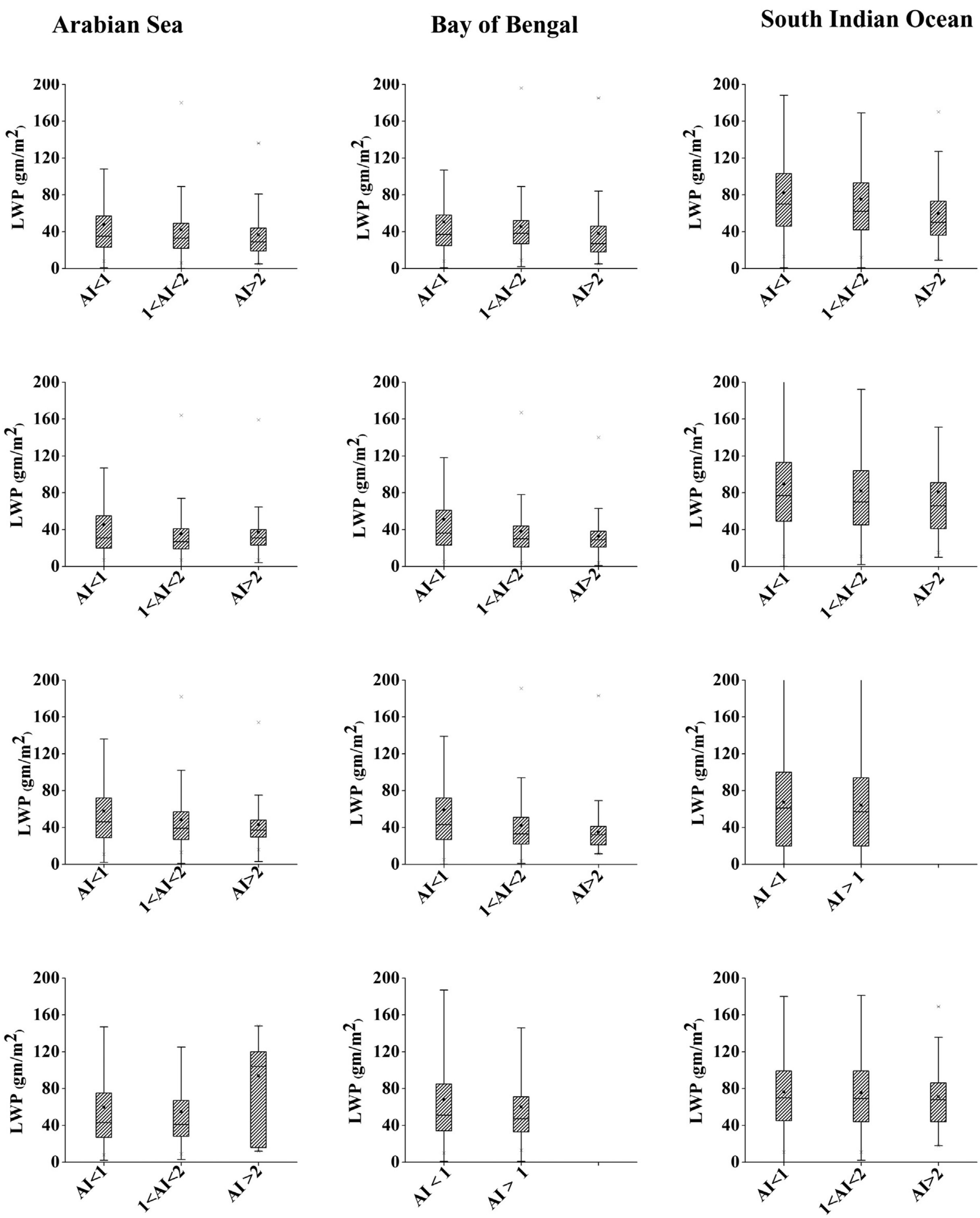

Fig. 6. Variation of LWP (g m^{-2}) with an increase in AI in the three regions. The panels from the top represent winter, pre-monsoon, monsoon and post-monsoon seasons. The error bars represent 5th–95th percentile ranges.

LWP bins but only in the range 150 < LWP < 350 g m^{-2} across the regions and seasons. However, the range of variation in R_{eff} across AOD bins is smaller in the SIO where AOD is lower compared to the AS and BoB. At lower LWP bins, even if fewer CCNs are available in clean condition, their growth is inhibited. At high LWP bins, no matter how many CCNs are available, there is enough moisture to facilitate cloud droplet growth (Sorooshian et al., 2010). In the middle range (150–350 g m^{-2}), cloud microphysics shows the highest sensitivity to an increase in aerosol loading. Fourthly, the reduction in R_{eff} at every LWP bin in the range 150–350 g m^{-2} with an increase in AOD is not statistically significant uniformly. The aerosol signal is most prominent in the post-monsoon to winter seasons. Also, the signal is strong when AOD increases from < 0.1 to the next higher bin in all the seasons. Further increase in AOD beyond 0.3 does not show a significant decrease in R_{eff} in this LWP range. Earlier studies demonstrated cloud invigoration by aerosol forcing in the Indian monsoon region (e.g.

Sengupta et al., 2013; Sarangi et al., 2017), where clouds start growing vertically rapidly in presence of high aerosol loading as warm rain is suppressed initially. This would in turn increase R_{eff}, and hence would compete with indirect effect (where R_{eff} is expected to decrease). Lastly, the range of variation of R_{eff} across a widely varying LWP is lower in the winter season relative to the other seasons mainly in the AS and BoB when the anthropogenic fraction is higher in the aerosol load. All these results strongly point towards aerosol indirect effect as it is not possible to explain these observations solely by meteorology or by retrieval artifacts. In fact, our analysis discloses the meteorological (increasing R_{eff} with increasing LWP) as well as aerosol (lower R_{eff} at higher AOD across LWP bins) signals simultaneously.

3.3. Probable evidence of aerosol semi-direct effect

Aerosol semi-direct effect where moisture inside the clouds gets evaporated due to aerosol-induced heating was first discovered in the INDOEX (Ackerman et al., 2000), which was conducted in the winter season over the northern Indian Ocean (covering the AS and BoB). Here we examine whether the signal of semi-direct effect can be detected in the other seasons too by analyzing the changes in LWP with an increase in absorbing aerosols (quantified by AI). First, we report monthly climatology of AI over the three oceanic regions (Fig. 5). AI shows a feeble seasonality over the SIO with slightly higher AI in the month of October and November, which may be attributed to biomass burning aerosols transported from the Indonesian peninsula (Lestari et al., 2014). On the contrary, the fraction of absorbing aerosols increases over the AS and BoB during the pre-monsoon and monsoon seasons. Dust is transported from the Indian desert and middle-eastern deserts to the BoB via IGB and along the west coastline of India (Dey and DI Girolamo, 2010) during the pre-monsoon season. Dust is transported to the AS not only in this season, but it continues in the monsoon season also reaching a peak in June–July (Dey and Di Girolamo, 2010). Due to the proximity to the dust source regions, larger AI is observed over the AS compared to the BoB with SIO showing the least values.

Next, we show the variation of LWP with an increase in AI in all the three regions in the winter season (Fig. 6). We note that AI > 2 bin over the SIO has fewer samples than the other two bins and hence the statistics have low sampling bias. In the pre-monsoon season when the aerosol load is dominated by dust (that is moderately absorbing), a similar variation in LWP is observed in all the three oceanic regions. In the monsoon season also, the signal is visible in the AS and BoB only and not detectable in the post-monsoon season in any of these regions. Also, the reduction is larger from $AI < 1$ to $1 < AI < 2$ bin than from $1 < AI < 2$ to $AI > 2$ bin. This is perhaps because even though AI is high (implying higher fraction of absorbing aerosols), overall aerosol loading is too low to have any significant impact that can be discernible.

4. Discussion and conclusions

In this work, we analyze the variations of marine water cloud properties (f_c, R_c, LWP, and R_{eff}) with an increase in AOD and AAI over the oceanic regions adjacent to the Indian subcontinent using 15 years of satellite observations. Though satellite aerosol and cloud products are more accurate over the oceans than over the land, it is prudent to discuss a few issues that impact signal of aerosol-cloud interaction. Liang et al. (2015) have shown that MODIS R_{eff} is biased high in the tropical oceans. If this is true, the aerosol signal reported here is perhaps conservative, especially in the AS and BoB during the post-monsoon and winter season when the marine water clouds are mostly trade-cumulus. Secondly, any correlation in aerosol and cloud parameters may not be causal and can be mediated by meteorology (Gryspeerdt et al., 2016). Hence rather seeking correlations between AOD and cloud parameters, we examine the changes in cloud properties (in relation to each other) with increasing AOD in the continuum. A similar pattern in each season reveals that aerosol indirect effect signal can be identified vis-à-vis the meteorological signal simultaneously in the oceans adjacent to the Indian subcontinent. Our study establishes consistency of aerosol impact on cloud characteristics in the Indian Ocean, which was previously demonstrated only in the winter season (Heymsfield and McFarquhar 2000; Ramanathan et al., 2001; Chylek et al., 2006; Dey et al., 2011). Since we restrict our analysis only to low clouds (CTP lower than 680 hPa), the signal of cloud invigoration (e.g. Sengupta et al., 2013; Sarangi et al., 2017) is not possible to detect and hence we do not show any analysis of CTP-AOD. We also observe probable evidence of the semi-direct effect. The key conclusions are as follows.

1. Cloud properties show stronger seasonality in the AS and BoB than in the SIO.
2. In the AS and BoB where AOD is > 0.2 throughout the year, R_{eff} is mostly confined within 14–19 μm, while it is higher (in the range 18–21 μm) in the SIO where AOD remains lower than 0.2.
3. Aerosol second indirect effect (i.e. smaller cloud drop size in polluted condition) is most prominent in the LWP range 150–350 $g\,m^{-2}$.
4. Cloud drops grow at a faster rate with an increase in LWP in the clean condition than in the polluted condition. Aerosol indirect effect signal saturates after AOD increases beyond 0.3.
5. Aerosol semi-direct effect seems to be evident in the AS and BoB in all the seasons except the post-monsoon season, when LWP is found to decrease with an increase in AOD.

Acknowledgements

The first author thanks IIT Delhi for providing PhD fellowship. We acknowledge NASA DAAC for archiving and distributing MODIS data. SD acknowledges DST-FIST program (SR/FST/ESII-016/2014) for providing computing support. We thank the anonymous reviewers for constructive comments that helped improving the original version of the manuscript.

References

Ackerman, A.S., Toon, O.B., Stevens, D.E., Heymsfield, A.J., Ramanathan, V., Welton, E.J., 2000. Reduction of tropical cloudiness by soot. Science. 288, 1042–1047.

Albrecht, B., 1989. Aerosols, cloud microphysics, and fractional cloudiness. Science. 245, 1227–1230.

Altaratz, O., Koren, I., Remer, L.A., Hirsch, E., 2014. Review: Cloud invigoration by aerosols- coupling between microphysics and dynamics. Atmos. Res. 140–141, 38–60. https://doi.org/10.1016/j.atmosres.2014.01.009.

Boucher, O., et al., 2013. Clouds and Aerosols. In: Climate Change: The Physical Science Basis. Contribution of Working Group I to the Fifth Assessment Report of the Intergovernmental Panel on Climate Change (IPCC 5). Cambridge University Press, Cambridge, United Kingdom and New York, NY, USA.

Cherchi, A., Gualdi, S., Behera, S., Luo, J.J., Masson, S., Yamagata, T., Navarra, A., 2007. The influence of tropical Indian Ocean SST on the Indian summer monsoon. J. Clim. 20, 3083–3105.

Christensen, M.W., Neubauer, D., Poulsen, C.A., Thomas, G.E., McGarragh, G.R., Povey, A.C., Proud, S.R., Grainger, R.G., 2017. Unveiling aerosol–cloud interactions—Part 1: Cloud contamination in satellite products enhances the aerosol indirect forcing estimate. Atmos. Chem. Phy. 17 (21), 13151–13164.

Chylek, P., Dubey, M.K., Lohmann, U., Ramanathan, V., Kaufman, Y.J., Lesins, G., Hudson, J., Altmann, G., Olsen, S., 2006. Aerosol indirect effect over the Indian Ocean. Geophys. Res. Lett. 33, L06806. https://doi.org/10.1029/2005GL025397.

Dey, S., Di Girolamo, L., 2010. A climatology of aerosol optical and microphysical properties over the Indian Subcontinent from 9 years (2000-2008) of Multiangle Imaging Spectro Radiometer (MISR) data. J. Geophys. Res. 115, D15204. https://doi.org/10.1029/2009JD013395.

Dey, S., Larry, D.J., Zhao, G., 2011. Satellite-observed relationships between aerosol and trade-wind cumulus cloud properties over the Indian Ocean. Geophys. Res. Lett. 38, L01804. https://doi.org/10.1029/2010GL045588.

Duflot, P., Royer, P., Chazette, P., Baray, J.L., Courcoux, Y., Delmas, R., 2011. Marine and biomass burning aerosols in the southern Indian Ocean: Retrieval of aerosol optical properties from shipborne lidar and Sun photometer measurements. J. Geophys. Res.Atmospheres 116, D18. https://doi.org/10.1029/2011JD015839.

Eck, T.F., et al., 2012. An analysis of AERONET aerosol absorption properties and classifications representative of aerosol source regions. J. Geophys. Res. 117 (D17). https://doi.org/10.1029/2012JD018127.

Fan, J., Wang, Y., Rosenfeld, D., Liu, X., 2016. Review of aerosol–cloud interactions:

mechanisms, significance, and challenges. J. Atmos. Sci. 73 (11), 4221–4252.
Google maps, 2019. https://www.google.com/maps/place/Indian+Ocean/.
Gryspeerdt, E., Quass, J., Bellouin, N., 2016. Constraining the aerosol influence on cloud fraction. J. Geophys. Res. 121, 3566–3583. https://doi.org/10.1002/2015JD023744.
Hansen, J., Sato, M., Kharecha, Russell, Lea, D.W., Siddall, M., 2007. Climate change and trace gases. Philos. Trans. R. Soc. Lond. A 365, 1925–1954.
Heymsfield and McFarquhar, 2000. Microphysics of INDOEX clean and polluted trade cumulus clouds. J. Geophys. Res. 106 (D22), 28,653–28,673.
Johnson, B.T., Shine, K.P., Forster, P.M., 2004. The semi-direct aerosol effect: Impact of absorbing aerosols on marine stratocumulus. Quart. J. Royal Met. S. 130, 1407–1422. https://doi.org/10.1256/qj.03.61.
Kant, S., Panda, J., Gautam, R., 2019a. A seasonal analysis of aerosol-cloud-radiation interaction over Indian region during 2000-2017. Atmos. Environ. 201, 212–222. https://doi.org/10.1016/j.atmosenv.2018.12.044.
Kant, S., Panda, J., Pani, S.K., Wang, P.K., 2019b. Long-term study of aerosol–cloud–precipitation interaction over the eastern part of India using satellite observations during pre-monsoon season. Theor. Appl. Clim. 136, 605–626.
King, M.D., Tsay, S.C., Platnick, S.E., Wnag, M., Liou, K.N., 1997. Cloud Retrieval Algorithms for MODIS: Optical Thickness, Effective Particle Radius, and Thermodynamic Phase. MODIS Algorithm Theoretical Basis Document. Goddard Space Flight Center, NASA, USA.
Kulkarni, J.R., et al., 2012. The Cloud Aerosol Interactions and Precipitation Enhancement Experiment (CAIPEEX): Overview and preliminary results. Curr. Sci. 102 (3), 413–425.
Lauer, A., Hamilton, K., 2013. Simulating clouds with global climate models: a comparison of CMIP5 results with CMIP3 and satellite data. J. Clim. 26, 3823–3845. https://doi.org/10.1175/JCLI-D-12-00451.1.
Lestari, R.K., Watanabe, M., Imada, Y., Shiogama, H., Field, R.D., Takemura, T., Kimoto, M., 2014. Increasing potential of biomass burning over Sumatra, Indonesia induced by anthropogenic tropical warming. Environ. Res. Lett. 9, 104010.
Levy, R.C., mattoo, S., Munchk, L.A., Remer, L.A., Sayer, A.M., Patadia, F., Hsu, N.C., 2013. The collection 6 MODIS aerosol products over land and ocean. Atmos. Measur. Tech. 6, 2989–3034.
Li, Z., et al., 2016. Aerosol and monsoon climate interactions over Asia. Rev. Geophys. 54 (4), 866–929.
Liang, L., Girolamo, L.D., Sun, W., 2015. Bias in MODIS cloud drop effective radius for oceanic water clouds as deduced from optical thickness variability across scattering angles. J. Geophys. Res. 120 (15). https://doi.org/10.1002/2015JD023256.
Liu, Y., et al., 2017. Analysis of aerosol effects on warm clouds over the Yangtze River Delta from multi-sensor satellite observations. Atmos. Chem. Phy. 17 (9), 5623–5641.
Minnis, P., Ayers, J.K., Palikonda, R., Phan, D., 2004. Contrails, cirrus trends, and climate. J. Clim. 17, 1671–1685.
Moorthy, K.K., Babu, S.S., Manoj, M.M., Satheesh, S.K., 2013. Buildup of aerosols over the Indian Region. Geophys. Res. Lett. 40, 1011–1014. https://doi.org/10.1029/2012GL054876.
Noh, Y.C., Sohn, B.J., Kim, Y., Joo, S., Bell, W., 2016. Evaluation of temperature and humidity profiles of Unified Model and ECMWF analyses using GRUAN radiosonde observations. Atmosphere 7, 1–13.
Pandithurai, G., 2012. Aerosol effect on droplet spectral dispersion in warm continental cumuli. J. Geophys. Res. 117, D16202. https://doi.org/10.1029/2011JD016532.
Platnick, S., et al., 2017. The MODIS cloud optical and microphysical products: Collection 6 updates and examples from Terra and Aqua. IEEE Trans. Geosci. Remote Sensing 55 (1), 502–525.
Ramanathan, V., et al., 2001. The Indian Ocean Experiment: an integrated assessment of the climate forcing and effects of the Great Indo-Asian haze. J. Geophys. Res. 106, 28371–28399.
Remer, L.A., et al., 2005. The MODIS aerosol algorithm, products, and validation. J. Atmos. Sci. 62, 947–973.
Rosenfeld, D., 1999. TRMM observed first direct evidence of smoke from forest fires inhibiting rainfall. Geophys. Res. Lett. 26, 3105–3108.
Rosenfeld, D., Sherwood, S., Wood, R., Donner, L., 2014. Climate effects of aerosol-cloud interactions. Atmos. Sci. 343 (6169), 379–380.
Sarangi, C., Tripathi, S.N., Kanawade, V.P., Koren, I., Pai, D.S., 2017. Investigation of the aerosol–cloud–rainfall association over the Indian summer monsoon region. Atmos. Chem. Phy. 17, 5185–5204.
Satheesh, S.K., Torres, O., Remer, L.A., Babu, S.S., Vinoj, V., Eck, T.F., Kleidman, R.G., Holben, B.N., 2009. Improved assessment of aerosol absorption using OMI-MODIS joint retrieval. J. Geophys. Res. 114, D05209. https://doi.org/10.1029/2008JD011024.
Sayer, A.M., Hsu, N.C., Bettenhausen, C., Lee, J., Redemann, J., Schmid, B., Shinozuka, Y., 2016. Extending “Deep Blue” aerosol retrieval coverage to cases of absorbing aerosols above clouds: Sensitivity analysis and first case studies. J. Geophys. Res. 121, 4830–4854.
Seinfeld, J.H., Pandis, S.N., 1998. Atmos. Chem. and Phy. John Wiley, New York, pp. 1326.
Seinfeld, J.H., et al., 2016. Improving our fundamental understanding of the role of aerosol-cloud interactions in the climate system. Proc. Natl. Acad. Sci. USA 113, 5781–5790. https://doi.org/10.1073/pnas.1514043113.
Sengupta, K., Dey, S., Sarkar, M., 2013. Structural evolution of monsoon clouds in the Indian CTCZ region. Geophys. Res. Lett. 40, 5295–5299.
Sorooshian, A., Fiengold, G., Lebsock, M.D., Jiang, H., Stephens, G.L., 2010. Deconstructing the precipitation susceptibility construct: improving methodology for aerosol-cloud precipitation studies. J. Geophys. Res. 115, D17201. https://doi.org/10.1029/2009JD013426.
Squires, P., Twomey, S., 1966. A comparison of cloud nucleus measurements over Central North America and the Caribbean Sea. J. Atmos. Sci. 23, 401–404.
Stevens, B., Feingold, G., 2009. Untangling aerosol effects on clouds and precipitation in a buffered system. Nature 461, 607–613. https://doi.org/10.1038/nature08281.
Tanré, D., et al., 1997. Remote sensing of aerosol properties over oceans using the MODIS/EOS spectral radiances. J. Geophys. Res. 102 (D14), 16971–16988. https://doi.org/10.1029/96JD03437.
Torres, O., Tanskanen, A., Veihelmann, B., Ahm, C., Braak, R., Nhartia, P.K., Veefkind, P., Levelt, P., 2007. Aerosols and surface UV products from ozone monitoring Instrument observations: an overview. J. Geophys. Res. 112, D24S47.
Wang, C., 2013. Impact of anthropogenic absorbing aerosols on clouds and precipitation: a review of recent progresses. Atmos. Res. 122, 237–249. https://doi.org/10.1016/j.atmosres.2012.11.005.
Warner, J., Twomey, S., 1967. The production of cloud nuclei by cane fires and the effect on cloud droplet concentration. J. Atmos. Sci. 24, 704–706.